WACS—Wide-Area Stability and Voltage Control System: R&D and Online Demonstration

CARSON W. TAYLOR, FELLOW, IEEE, DENNIS C. ERICKSON, FELLOW, IEEE, KENNETH E. MARTIN, SENIOR MEMBER, IEEE, ROBERT E. WILSON, SENIOR MEMBER, IEEE, AND VAITHIANATHAN VENKATASUBRAMANIAN

Invited Paper

As background, we describe frequently used feedforward wide-area discontinuous power system stability controls. Then we describe online demonstration of a new response-based (feedback) Wide-Area stability and voltage Control System (WACS). The control system uses powerful discontinuous actions for power system stabilization. The control system comprises phasor measurements at many substations, fiber-optic communications, real-time deterministic computers, and transfer trip output signals to circuit breakers at many other substations and power plants. Finally, we describe future development of WACS. WACS is developed as a flexible platform to prevent blackouts and facilitate electrical commerce.

Keywords*—*Blackout prevention, emergency control, phasor measurements, power system stability, unstable limit cycle, voltage stability, wide-area measurements and control.

I. INTRODUCTION

The Bonneville Power Administration (BPA), Portland, OR; Ciber Inc., Beaverton, OR; and Washington State University (WSU), Pullman, are designing and implementing a Wide-Area stability and voltage Control System termed *WACS*. WACS provides a flexible platform for rapid implementation of generator tripping and reactive power compensation switching for transient stability and voltage support of a large power system. Features include synchronized positive sequence phasor measurements, digital fiber-optic communications from 500-kV substations, a real-time control computer programmed in the G language, and output communications for generator tripping and 500-kV capacitor/reactor bank switching. The WACS software runs two algorithms in parallel.

As background, we describe widely used emergency controls termed Special Protection Systems (SPS). SPS is based on *direct detection* of predefined outages, with high-speed binary (transfer trip) signals to control centers for logic decisions, and then to power plants and substations for generator tripping and capacitor/reactor bank switching. Disadvantages of SPS include control for only predefined events, complexity, and relatively high cost.

In contrast with SPS, WACS employs strategically placed sensors to react to the power system *response* to arbitrary disturbances. WACS provides single discontinuous stabilizing actions or true feedback control. As true feedback control, the need for discontinuous action is determined and commanded, the power system response is observed, and further discontinuous action such as generator tripping or capacitor bank switching is taken as necessary. The WACS platform may also be used for wide-area modulation control of generators and transmission-level power electronic devices and for control center operator alarms and monitoring.

We describe WACS benefits and describe large-scale simulations showing the interarea stabilization of large disturbances by WACS.

We also describe WACS design (measurement, communications, control), and initial online implementation. Online testing results include statistics of communications delay from global positioning system (GPS) time-tagged substation measurements to GPS-timed receipt by the control computer.

Manuscript received May 3, 2002; revised October 25, 2003. The work at Washington State University was supported in part by the Power System Electric Engineering Research Center (PSERC) and in part by the Consortium for Electric Reliability Technology Solutions (CERTS).

C. W. Taylor and K. E. Martin are with the Bonneville Power Administration, Vancouver, WA 98666 USA (e-mail: cwtaylor@bpa.gov; kemartin@bpa.gov).

D. C. Erickson is with Ciber, Inc., Beaverton, OR 97007 USA (e-mail: derickson@ciber.com).

R. E. Wilson is with Western Area Power Administration, Lakewood, CO 80228 USA (e-mail: rewilson@wapa.gov).

V. Venkatasubramanian is with the Department of Electrical and Computer Science, Washington State University, Pullman, WA 99165 USA (e-mail: mani@eecs.wsu.edu).

Digital Object Identifier 10.1109/JPROC.2005.846338

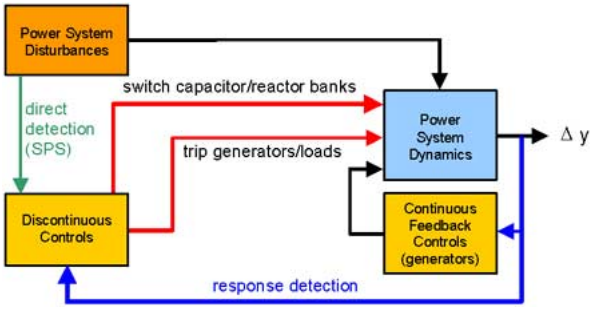

Fig. 1. Local and wide-area, continuous and discontinuous power system stability controls. Adapted from drawings by Dr. J. F. Hauer.

II. Power System Stability Controls

Power system stability controls are described in several books and reports [1]–[5]. Reference [6] is an early, but still valuable, paper describing discontinuous controls.

Fig. 1 shows a block diagram of the power system stability control environment. Power system stability encompasses electromechanical (rotor angle) stability among groups of synchronous generators, and voltage stability involving load response to disturbances [7]. RMS-type sensors are generally used—electromechanical oscillations and slow voltage variations amplitude-modulate the 50- or 60-Hz power frequency waveforms. Electromagnetic transients are not of primary interest except for sensor filtering considerations.

Most stability controls are continuous feedback controls at power plants: automatic voltage regulator and power system stabilizer for generator excitation control, and prime mover control (speed governor). Controls are largely the single-input–single-output type, designed via classical feedback control methods [1]. Additional local continuous stability controls are at transmission-level power electronic devices such as static var compensators. There are also local discontinuous controls for reactive power compensation (capacitor/reactor banks) switching and load shedding.

Installed wide-area stability controls are mainly based on direct detection of selected outages. These emergency controls are termed SPS or remedial action schemes. We describe these controls in Section IV.

Advanced wide-area stability controls measure power system response to disturbances. There are very few implementations at present. We describe present-day projects in Sections V and VI.

Discontinuous controls supplement the basic continuous controls by relieving stress for very large disturbances, providing a region of attraction and a secure postdisturbance operating or equilibrium point. Continuous controls then operate effectively over a smaller nonlinear range.

Wide-area controls—feedforward and feedback, continuous and discontinuous—obviously have potential for improved observability and controllability.

III. Western North American Power System

Fig. 8 in Section VI shows the western North American interconnected power system. Connections to the eastern North American synchronous interconnection are by small back-to-back HVdc converter stations.

Long-distance interarea transmission lines characterize the western interconnection. Major lines are 500-, 345-, and 230-kV. There are two ±500-kV dc links: the 3100-MW 1360-km Pacific HVdc intertie from the Columbia River to Los Angeles and the 1920-MW 787-km Intermountain Power Project link from Utah to southern California. Hydro power predominates in the Pacific Northwest (PNW—British Columbia, Washington State, and Oregon). Large coal-based power plants predominate in the eastern and southern portions of the interconnection. Most generation in California is natural gas or oil based.

In spring and summer, with good hydro generation conditions, the dominant interarea power flows are from the PNW to California and also from coal-based generation in the eastern areas (Wyoming, Utah, Arizona, and Nevada) to California. The northern California portion of the Pacific ac intertie comprises three series capacitor compensated 500-kV lines with nonsimultaneous rating of 4800 MW for the three Oregon to California lines.

Large-scale power flow and transient stability simulations of potential disturbances are necessary to determine transfer limits for many defined transmission paths. Power flow (steady-state) simulations model over 10 000 buses (nodes representing generation and load injection stations, and transformer substations), requiring solving over 20 000 nonlinear algebraic equations. Transient stability simulation adds thousands of nonlinear differential equations. In defining simultaneous power transfer limits, major sensitivities are shown on nomograms. Portions of nomogram boundaries are limited by either first swing transient stability, transient damping of oscillations, or postdisturbance voltage support criterion.

Controls described in this paper are oriented toward high-power transfers from the PNW and British Columbia to California, but are adaptable to other applications.

IV. Feedforward Wide-Area Stability Controls

The widely used SPS provide control for potential single and multiple-related outages identified in the power system planning process. Compared to the financial and permitting difficulties of transmission line construction, SPS are low cost and easy to install. A large increase in power transfer capability is realized.

As generation and load increase without corresponding increase in transmission lines, SPS controls proliferate [8]. At BPA, there are many schemes for a myriad of operating and disturbance conditions. Tens of millions of dollars have been invested over many years. Additional schemes were added following the cascading power failures in summer 1996 [9], [10].

Control actions are mainly for detection of transmission outages, but also for some generation outages. The most complex scheme involves the Pacific ac intertie where high-speed outage detection of around fifty 500-kV lines is installed (detection at both line ends). Fault tolerant

programmable logic controllers are at BPA's two control centers: one near Portland and the other in Spokane, WA. The most important control action is tripping of PNW hydroelectric generators. There are few difficulties with tripping hydro generators and they can be rapidly returned to service. The generators are at the sending end of the PNW to California power transfer path, with the generator tripping braking remaining Northwest generators that are accelerating relative to southwest generators. For outages of either the Pacific ac or HVdc intertie, up to 2700 MW of generation may be tripped.

Other control actions are energizing 500-kV series and shunt capacitor banks, and disconnecting shunt reactors. BPA 500-kV shunt capacitor banks are in the 200–380 MVAr range.

Control actions take place as fast as 150 ms after the outage. The delay time includes detection time, communications to central logic, logic computer processing time, communications to power plants and substations, and power circuit breaker operating time. Communication of SPS activation signals use the same high-speed "transfer trip" used for isolation of transmission line short circuits. At BPA these are primarily frequency shift key audio tones over analog microwave. Newer systems use digital messages over digital microwave or fiber optics (SONET).

The consequences of SPS failure can be large-scale blackouts. Controls are clearly not as robust as additional transmission lines and must be highly reliable by design. High redundancy in detection, communication, and logic computers is required.

The complexity of the SPS is ever increasing. BPA has a full-time operator devoted to prearming (enabling) and monitoring the many schemes.

Besides complexity, a shortcoming of preplanned event driven control is that other disturbances may occur that have not been considered in planning. These may originate in other parts of the interconnected power system.

V. Feedback Wide-Area Stability Controls

Feedback controls measure power system variables and can respond to arbitrary disturbances. Control can be continuous or discontinuous.

Stability control using remote signals are not new and are a simplified form of wide-area control. In 1976, BPA implemented modulation of the Pacific HVdc intertie using active power and later current magnitude signals from a remote substation on the parallel Pacific ac intertie [11], [12]. The continuous control damped electromechanical oscillations between groups of PNW generators and groups of Pacific Southwest generators; the oscillation period was around 3 s. Analog microwave communications and analog controls were used. The modulation was single input–four outputs, the outputs being active and reactive power at the northern HVdc terminal (rectifier operation) in Oregon and active and reactive power at the southern terminal (inverter operation) near Los Angeles. Modulation was discontinued after a major expansion of the HVdc intertie from two terminals to four terminals in 1989.

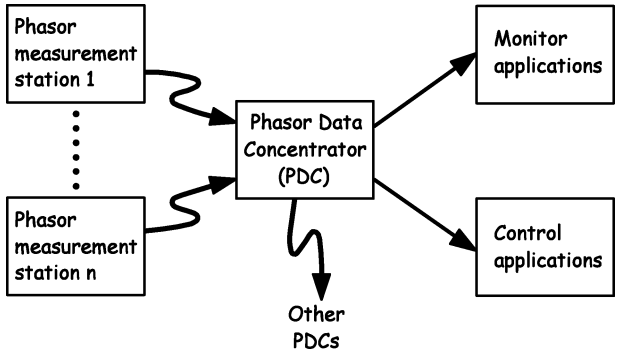

Fig. 2. Control center PDC.

A. Phasor Measurements

Although various types of rms sensors may be used, digital positive sequence, GPS-synchronized phasor measurements [4], [5], [13], [14] are most often considered for wide-area control. "Positive sequence" refers to transformation of an unbalanced set of three-phase voltages or currents into a set of positive, negative, and zero sequence "symmetrical components," where positive sequence is a set of three-phase voltages or currents with equal magnitudes, 120° phase difference, and normal phase rotation [5, Ch. 8]. In normal operation without short circuits or individual phase outages, the phase voltages and currents are nearly equal to the positive sequence voltages and currents.

Several manufacturers offer phasor measurement sensors. Typically, channels for multiple three-phase voltage and current measurements are provided. The positive sequence voltage and current phasors are computed and GPS time tagged once every two cycles, or in newer equipment, once every cycle of the power frequency (30- or 60-Hz data rate for 60-Hz power frequency). Power system frequency deviation from nominal is also computed, with GPS providing a precise time and frequency reference. There are tradeoffs between response speed and filtering. The phasor measurements are grouped, and data packets are transmitted to a central site where packets from several measurement locations (substations) are organized by time stamp [15], [16]. Outputs from a "phasor data concentrator" (PDC) are networked to monitoring and control applications (Fig. 2).

From the voltage and current phasors, applications may compute active and reactive power.

In coming years, phasor measurements will become more common as part of IT advances such as substation automation. The phasor measurements can be made available at small cost as part of other substation measurements, for example, protective relaying [17].

Networked phasor measurements are a key part of a BPA/U.S. Department of Energy/Electric Power Research Institute (EPRI)/Western Area Power Administration program for wide-area measurement systems (WAMS) [5, Ch. 11.8], [18]. WAMS is valuable for power system identification, power system monitoring, control center state

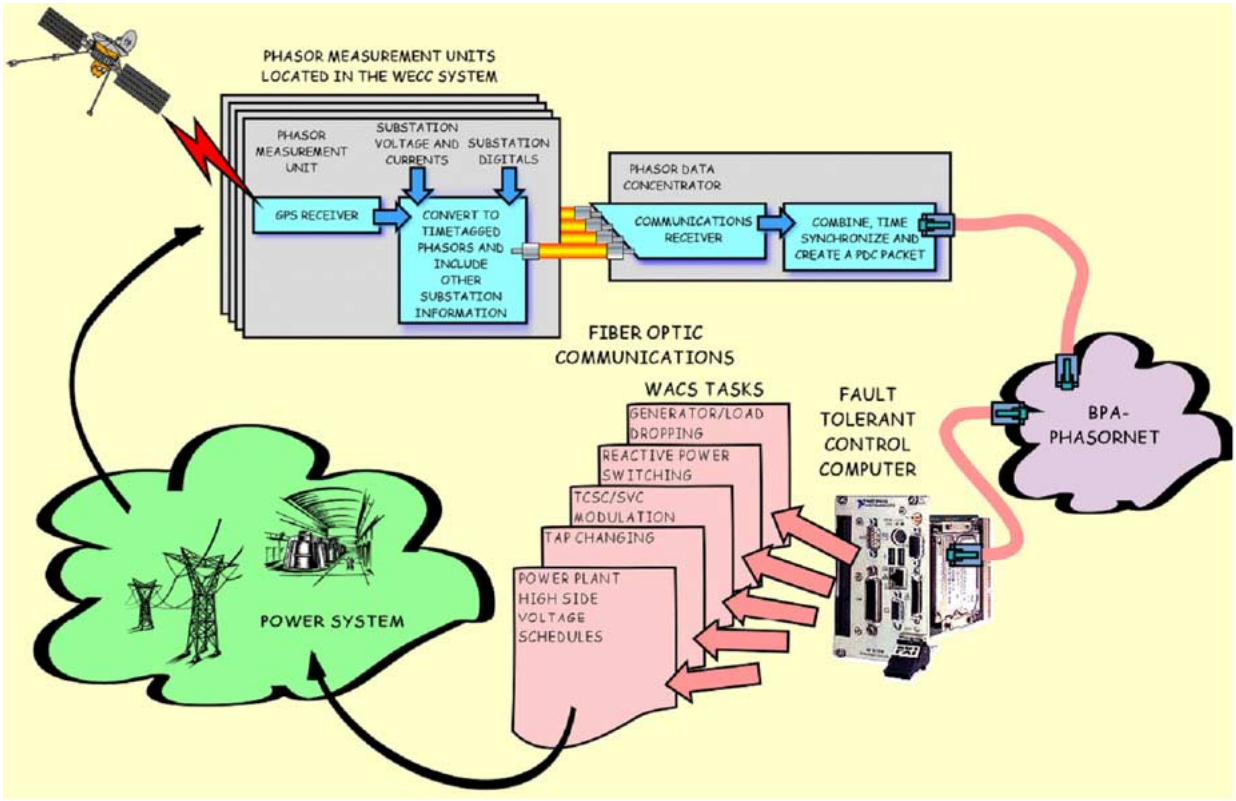

Fig. 3. WACS block diagram.

estimation, and power system dynamic performance analysis following disturbances—including large blackouts.

B. Continuous Wide-Area Controls

Continuous wide-area controls offer observability and controllability benefits where conventional local continuous controls have shortcomings. Possibilities include "wide-area power system stabilizers" [19] and controls for powerful transmission-level power electronic devices such as HVdc, thyristor-controlled series capacitors, and static var compensators.

Wide-area controls are especially attractive for unusual system structures. Remote signals may augment control using local measurements.

Because of increased control leverage and continuous exposure to adverse interactions, caution compared to local control is required. Communications latency is one concern. Dynamics mimicking electromechanical oscillations are another [20], [21]. These may include sensor processing artifacts such as aliasing of network resonances or harmonics, or generator shaft torsional dynamics. Hydro plant water column oscillations may appear to be electromechanical oscillations. Extra monitoring and supervision of control is desirable.

C. Discontinuous Wide-Area Controls

Compared to continuous control, discontinuous control tends to be safer—action is only taken when necessary. Discontinuous control has similarities with biological systems where stimuli must be above an activation threshold.

Similar to feedforward controls (SPS), feedback discontinuous controls initiate a large stabilizing action that improves first swing transient stability, reduces stress to improve oscillation damping, and provides a larger region of attraction for a more secure postdisturbance operating point.

We next describe a specific wide-area discontinuous feedback control (WACS) in development and demonstration.

VI. WACS

A. Overview

Fig. 3 shows a pictorial block diagram of WACS. Selected existing phasor measurements are used for inputs, and existing SPS transfer trip circuits are available for outputs. The new development is the real-time controller.

Based partly on the 10 August 1996 cascading failure [10], the original BPA concept was to combine voltage magnitude measurements with generator reactive power measurements using fuzzy logic. The premise is that generator reactive power measurements can be a more sensitive indicator of insecurity than voltage magnitude—voltages can be near normal but generator reactive power outputs near limits indicate insecurity. R&D at WSU showed, however, that a voltage magnitude based control is faster and simpler for transient stability [22]. Both methods are now used. Recent field experience has actually shown that the two methods, Vmag and Vmag$Q$ algorithms, have similar speed. This is partly due to recent replacement of slow rotating generator field winding excitation equipment with modern thyristor exciters at two large power plants.

References [23]–[25] describe recent WACS research and development.

Twelve voltage magnitude measurements from seven 500-kV stations are used. Two stations are near the Oregon–California border (Malin and Captain Jack), one is in central Oregon (Summer Lake), and three are near the Columbia River in northern Oregon or southern Washington (John Day, Slatt, Ashe, and McNary). Fifteen generator reactive power measurements at five power plant switching stations near the Columbia River are used (Big Eddy, John Day, Slatt, Ashe, and McNary). The hydro power plants feeding into Big Eddy, John Day, and McNary comprise 18, 16, and 12 generators, respectively; two to four generators are connected to a transmission line from the power plant to the switching station where phasor measurements are made.

We designed WACS so that loss of measurements from a single location or even multiple locations will only slightly degrade control. Measurements at widely spaced locations (hundreds of kilometers) provide spatial averaging or filtering against the aliasing effects discussed above. Spatial filtering along with discontinuous control action biases the phasor measurement requirements toward fast response rather than secure filtering.

B. Allowable Time for Control Actions

For first swing transient stability, control action must be taken prior to the peak of the forward interarea angle swing—the sooner the better. For a simple second-order undamped dynamic system with natural frequency of 1/3 Hz (3-s period), the step response peak is at 1.5 s. The impulse response peak is at 0.75 s. Most disturbances are closer to a step response than an impulse (the rare three-phase short circuit approaches an impulse, but opening the faulted line provides a step response effect). Nowadays the frequency of the Pacific intertie mode is around 0.25 Hz (4-s period), allowing more time for control action. The oscillation frequency is even lower for high-stress operation.

For transient stability, control action should be completed within around 1 s—especially for the less powerful capacitor/reactor bank switching.

The delay time for phasor measurement, fiber-optic communications, PDC throughput including wait time for slowly arriving packets, transfer trip, and circuit breaker tripping (of generators or shunt reactors) or closing (shunt capacitor bank insertion) are approximately 3, 2, 2, 1, and 2–5 60-Hz cycles respectively, or around 10 cycles for tripping and 13 cycles for closing (167 and 217 ms). Time for several control execution loops, intentional time delay, and throughput delay will be 67 ms or longer. Thus, it appears that control action can be taken within 0.3 s after sufficient power system electromechanical response to the disturbance. For capacitor/reactor bank switching, the local supervising voltage measurement sensors will be responding during the same time as the WACS measurements and processing.

The more sensitive $V\text{mag}Q$ algorithm may operate following longer time frame dynamics. In fact, need for the existing SPS action is determined by power flow simulation of a point in time several minutes after the disturbance.

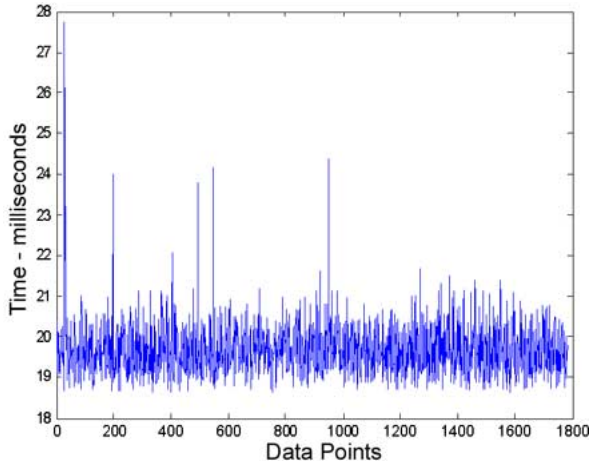

Fig. 4. Fiber-optic communications latency over 1 min, Slatt PMU to PDC.

The SPS helps ensure postdisturbance voltage support for angle stability following generator overexcitation limiting, tap changing, and other slower actions. Many seconds are available for taking sequential feedback actions as necessary.

The conditions existing in northeastern Ohio preceding the 14 August 2003 blackout were exactly what the $V\text{mag}Q$ algorithm caters to. Voltage magnitudes were mildly depressed, but Cleveland-area generators were at or near their reactive power limits [26]. Automatic load shedding by control similar to WACS could have prevented the blackout.

C. Phasor Measurement Communications and PDC

BPA legacy communications is analog microwave. Transmission of phasor measurement packets using modems has high latency (60–100 ms) and relatively high dropout rates. Thus, BPA-owned fiber-optic communications (SONET) are used for WACS. BPA has an extensive fiber-optic network, with links and terminal equipment still being added.

Fig. 4 shows tests of fiber-optic latency of less than 26 ms for a link from the Slatt switching station to a BPA control center. The link uses direct digital transfer into SONET.

D. Real-Time Hardware and Software

We selected National Instruments' LabVIEW Real-Time (RT) hardware and software [27]. The software is a true dataflow language that prevents race conditions and allows for parallel tasking (multitasking and multithreading are supported). It has many needed programming features and library components, including data acquisition/processing/output, TCP/UDP, signal processing, filtering, math operations, execution logic and state machine, execution tracing and timing, display graphics, and fuzzy logic tools with graphical editors. The graphical code is largely self-documenting. Modular architecture aids the testing and certification of critical modules by designing virtual simulated "real-world" conditions around them.

Controller development is done on a PC, and code is then downloaded to real-time deterministic hardware and software [27]. Fig. 5 shows the rack-mounted WACS hardware. A full-featured host PC that connects via Ethernet to the WACS RT engine is available to monitor, test, develop, and

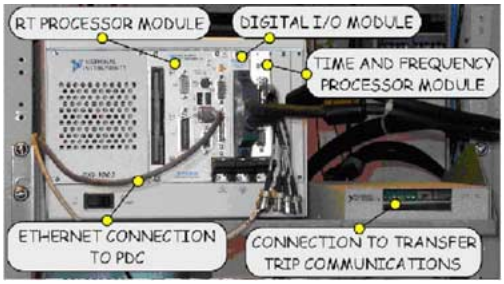

Fig. 5. WACS real-time hardware.

upload software and to run model studies for tuning. This is important, as the RT processor (engine) itself is always operated "headless" (no monitor, keyboard, or mouse). We do use a small text display status monitor and a sequence of events recorder.

WACS parameters are managed using an .ini file. This allows easy changes to the application for tuning the algorithms, defining station names, scale factors, etc. This is important in avoiding the pitfalls of "hardwiring."

1) Control Execution Rate: The rate at present is 30 control executions per second (33.3–ms intervals), which is the same rate as the phasor measurement packets. The time for a control execution cycle is around 8 ms, allowing addition of other features and moving to a future 60 packets per second data rate. For security against inadvertent actions during faults, measurement noise, and other disturbances, output must be above a threshold for two or more control executions.

2) Input Processing: Tasks include reading and decoding the data from the UDP Ethernet connection to the PDC and data sanity checks for transmission errors, nonvalid data, missing packets, and extra long latency. Close coordination with PDC data processing is required, and a customized message of only the needed measurements is transmitted to WACS. For missing or corrupt data, there are two options: one is to block the data and not use it in the algorithm, and the second is to pad the data with the last valid packet for a few control executions. The former is used currently. Both fatal and nonfatal errors are managed and reports issued. Also, the data is weighted and limit tested before being passed to the algorithm subroutines. The WACS software can also run in a library mode using simulation data or archived data from the PDC as inputs to the algorithms. This validates performance, facilitating certification.

3) Output Processing: Following the algorithm computations, a pattern consisting of up to 32 isolated outputs is sent to a relay control stage, where several masking operations are done before passing to the transfer trip communications. Any fatal or nonfatal error will mask outputs, with a user-defined mask available to disable one or more outputs either temporarily or long term or to disable the results of either or both the fast or slow algorithms.

E. The Vmag Algorithm

The voltage magnitude based Vmag algorithm provides first swing transient stability stabilization and relieves stress

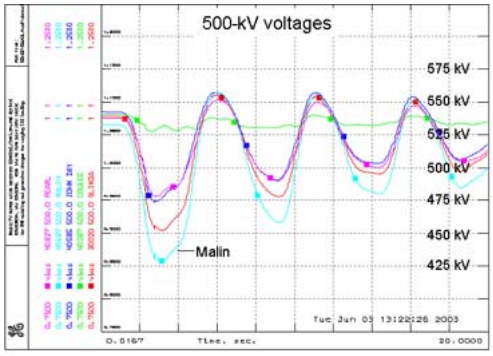

Fig. 6. BPA 500-kV voltages for outage of two Palo Verde generators with existing controls, with Pacific ac intertie loading of 4700 MW.

to improve transient damping. For growing oscillations, it will operate at some point for stabilization.

The algorithm is fairly simple, based on 12 voltage magnitude measurements at seven 500-kV stations. A weighted average voltage is computed from the 12 measurements, with highest weight for measurements close to the Oregon–California border where the voltage swings are usually greatest (Malin, Captain Jack, Summer Lake). A nonlinear accumulator (integrator) computes volt-seconds below a threshold setting that is currently 525 kV for capacitor/reactor bank switching and 520 kV for generator tripping (normal voltage is around 540 kV). Accumulation is blocked for voltage recovery. Control action results when the volt-second accumulation reaches a setpoint; also, the weighted voltage must be below 490 kV for generator tripping. The algorithm thus has semblance to proportional–integral (PI) control. Beneficially, faster operation results for more severe disturbances.

1) Critical Disturbance: A critical disturbance is near simultaneous outage of two nuclear generating units at a nuclear power plant in Arizona or California. Such events have occurred several times, and Western Electricity Coordinating Council (WECC) rules specify that cascading failure not result from these outages. Multigenerator outages at large coal-based power plants have also occurred.

The largest disturbance is outage of two nuclear generators at the Palo Verde nuclear plant near Phoenix, AZ. The combined power loss is around 2700 MW. The lost power is made up by inertia power from rotors of all other generators, and by response to decaying frequency by the speed governors of other generators. About half of the response comes from hydro generators in the northern half of the interconnected power system, resulting in a large increase in the Pacific ac intertie north to south loading. Instability (loss of synchronism between northern and southern generators) results if the initial intertie loading is high. There is no SPS for this outage.

2) Simulation of Two Palo Verde Generator Outages Without and With WACS: The Appendix describes simulation methodology. Fig. 6 shows 500-kV voltage responses for the two Palo Verde generator outages with existing controls. The initial Pacific ac intertie loading is 4700 MW. The largest voltage swing is at the Malin station near the Oregon–California border, and the performance is considered marginally acceptable.

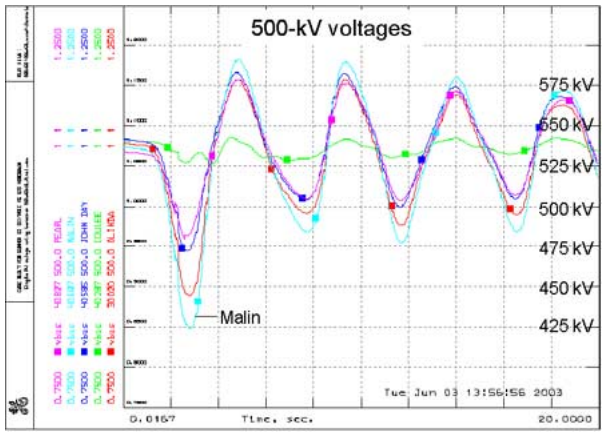

Fig. 7. BPA 500-kV voltages for outage of two Palo Verde generators with WACS and with Pacific ac intertie loading of 5000 MW.

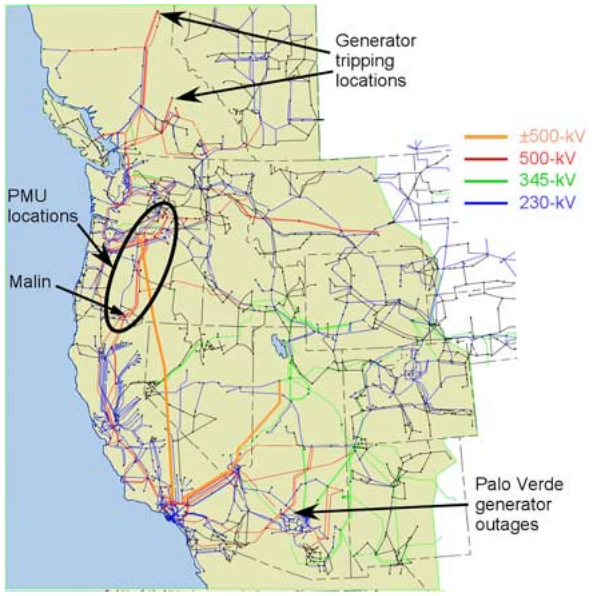

Fig. 8. Western North American interconnected power system showing disturbance location, and WACS input measurement locations and output action locations.

Fig. 7 shows similar response with WACS at an initial intertie loading of 5000 MW—a 300-MW gain. The main WACS action is 916 MW of generator tripping at two hydro power plants in British Columbia 1.4 s after the outage. WACS also inserted two 500-kV shunt capacitor banks 1.2 s after the outage. The transfer trip circuits from the BPA control center to the British Columbia power plants and capacitor bank locations exist as part of BPA's SPS. The higher oscillation frequency of Fig. 7 tends to indicate improved stability.

Fig. 8 shows the wide-area nature: an outage in Arizona, measurements in Oregon and southern Washington, and control actions in British Columbia.

3) Partial Failure of Measurements: Using the 5000-MW intertie loading with WACS case as reference, we simulate failure of the most important phasor measurement device. The failure is two voltage measurements at Captain Jack near Malin on the Oregon–California border. Simulation results are nearly identical to the reference case, so are not shown.

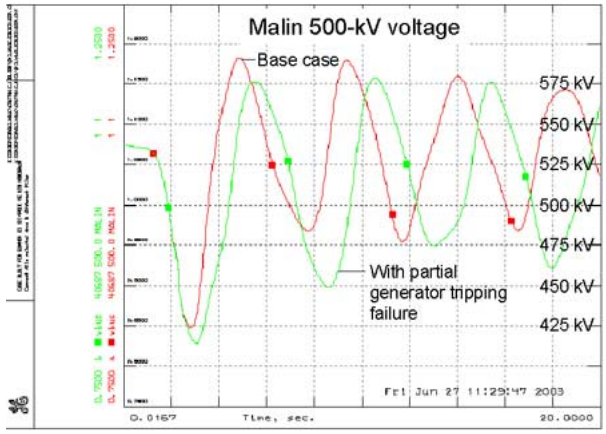

Fig. 9. Malin voltage for outage of two Palo Verde generators with partial failure of WACS generator tripping.

4) Partial Failure of Generator Tripping: Fig. 9 compares the reference case to simulation of failure of generator tripping at one of the two British Columbia power plants. Stability is maintained, but performance is notably degraded. The oscillation frequency decreases.

Other sensitivity cases lead to improved tuning of the algorithm. We simulate other outages to verify expected performance.

F. The VmagQ Algorithm

The VmagQ algorithm combines voltage magnitude measurements and generator reactive power measurements using fuzzy logic. Similar to the Vmag algorithm, we compute a weighted average 500-kV voltage magnitude from 12 phasor measurements at seven locations. More complicated is computation of weighted average reactive power from 15 transmission lines emanating from six large power plants. We compute active and reactive powers for these lines from the voltage and current phasors.

First, we estimate the number of connected generators—up to four generators per line may be connected on lines from hydro plants. While this information may be available at a slower data rate within a control center, we avoid interface and dependence on other data networks. The number of generators is estimated based on the normal loading range of individual generators. An error with estimation on one of the many lines is not serious.

A normalization procedure follows, based on generator active/reactive power capability curves. We map the capability curves from the generator terminals to the transmission side where the phasor measurement sensors are located, accounting for station service load, and generator step-up transformer impedance and tap ratio. Fig. 10 shows this one-time mapping for a large nuclear plant generator.

Normalization results in reactive power output on a scale of approximately ± 1 (generator controls allow large temporary and small steady-state operation outside limits). The transmission-side reactive power limits corresponding to the

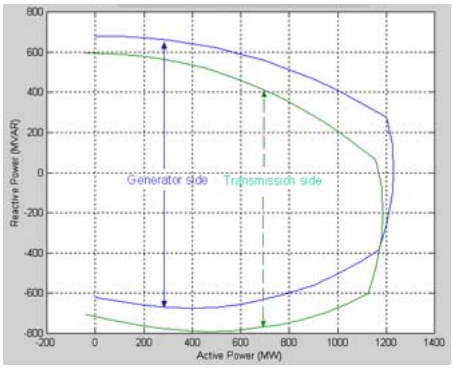

Fig. 10. Active/reactive power capability curve for a nuclear plant generator.

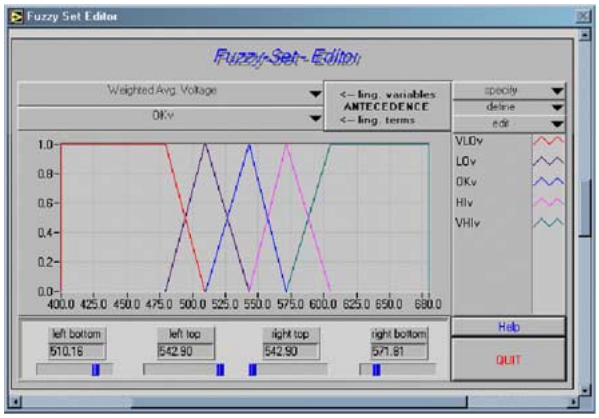

Fig. 11. Weighted average voltage fuzzy set input. Linguistic variables are VLOv (very low voltage), LOv (low voltage), OKv (OK voltage), HIv (high voltage), and VHIv (very high voltage).

active power are noted: $Q_{\max}$ and $Q_{\min}$. We compute the normalized value from transmission side values as follows:

$$Q_{\text{half}} = \frac{(Q_{\max} - Q_{\min})}{2}$$
$$Q_{\text{zero}} = Q_{\min} + Q_{\text{half}}$$
$$Q_{\text{norm}} = \frac{(Q - Q_{zero})}{Q_{\text{half}}}.$$

For example, for Fig. 10 with transmission side $P = 1000$ MW and $Q = 100$ MVAr, $Q_{\text{norm}} = 0.77$.

A weighted average of the normalized reactive powers is now computed. The individual weights are the product of the generator or generator group MVA rating and a factor. The factor is based on location and voltage support sensitivity. We give higher value to generators providing more sensitive control of transmission voltage by automatic voltage regulator line drop compensation [28] or by automatic high side voltage control.

We next combine the weighted average voltage magnitude and the weighted average generator reactive power are using basic fuzzy logic. To date, linguistic variable tuning is based on rules of thumb such as overlap cross points at 0.5. Figs. 11–13 show the input and output fuzzy sets. Fig. 14 shows the rule editor, and Fig. 15 shows the output control surface as a function of weighted average voltage for a weighted average generator reactive power input value of

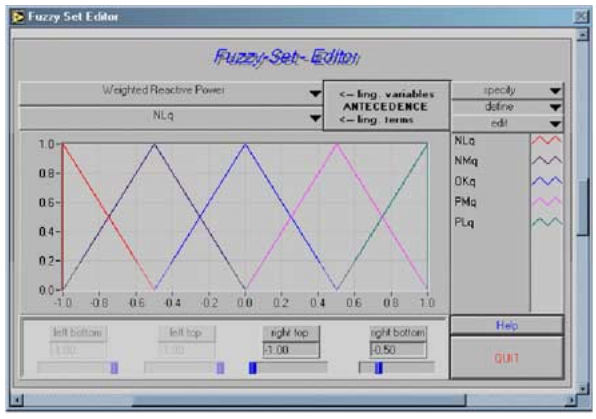

Fig. 12. Weighted average generator reactive power fuzzy set input. Linguistic variables are NLq (negative large reactive power), NMq (negative medium), Okq, PMq (positive medium), and PLq (positive large).

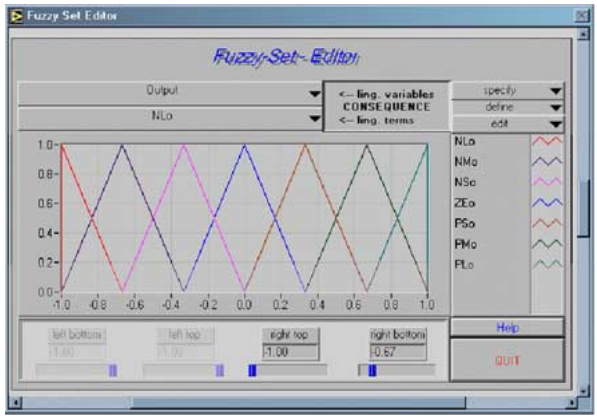

Fig. 13. Output (consequence) fuzzy set. Linguistic variables are NLo (negative large output), NMo (negative medium output), NSo (negative small output), ZEo (zero output), PSo (positive small output), etc.

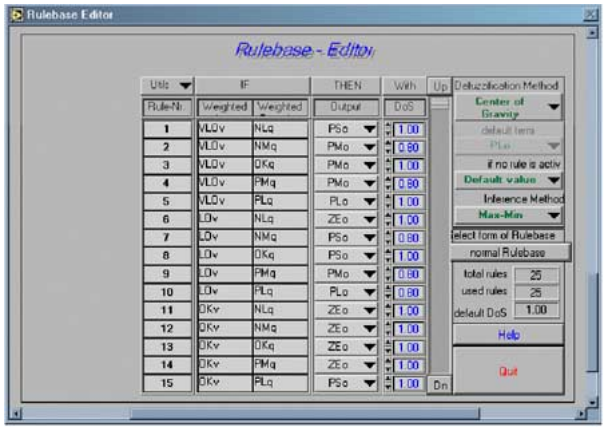

Fig. 14. Rule base. Output default value of zero if no rule is active. Center of gravity defuzzification method is selected. The MAX–MIN inference method is used, which is explained in the Fig. 15 caption for rule 8.

zero. The crisp output range is approximately ± 1, but elimination of unrealistic rule combinations result in a practical 0–1 range.

A crisp output value above a threshold enters an accumulator. With accumulator setpoint reached, capacitor/reactor

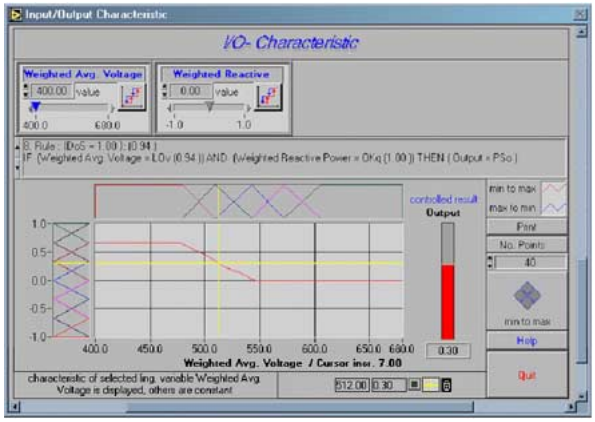

Fig. 15. Fuzzy controller voltage versus output characteristic for reactive power input of zero. At the cursor point, the voltage input is 512 kV, the output is 0.30, and rules 8 and 13 are active. As shown, Rule 8 fires with value of 0.94, which is MIN of the LOv and Okq linguistic variable values for 512-kV voltage and zero reactive power inputs (Figs. 11 and 12). For the output variable PSo, the area below 0.94 contributes to the center of gravity output (Fig. 13). If another rule activates output variable PSo, the MAX value of the two rules is used in the center of gravity computation.

Table 1
Power Flow Simulation Results, 4800 MW Intertie Power

	V_{Malin} kV	Q_{JohnD} MVAr	Vavg FL input	Qavg FL input	FL output
Pre outage	541.0	-158	540.7	0.273	0.10
2 Palo Verde outage	528.5	114	529.2	0.883	0.48
2 Palo Verde w/WACS[1]	530.5	89	533.7	0.826	0.45
2 Palo Verde w/WACS[2]	534.5	25	534.5	0.685	0.38

1 500-kV shunt capacitor/reactor bank switching at the 3 available locations.
2 Capacitor/reactor bank switching plus 500 MW generator tripping.

bank switching or generator tripping is commanded. Capacitor/reactor bank switching occurs first, with generator tripping only in more severe situations where capacitor/reactor bank switching is not available or not sufficient.

The main tuning is of the input measurement weights and the thresholds for output action—rather than the fuzzy sets.

As a power flow program steady-state simulation example, we simulated a simultaneous transfer nomogram limit point. Table 1 shows the fuzzy logic inputs and crisp outputs for a predisturbance case, the double Palo Verde outage case with existing controls, the outage case with WACS-initiated 500-kV capacitor/reactor bank switching at three locations, and the outage case with the capacitor/reactor bank switching and 500 MW of generator tripping. Also shown are key individual inputs to the fuzzy logic: voltage magnitude at Malin and reactive power from John Day power plant line 1 (John Day reactive power has the high weighting because of location and excellent voltage control performance).

The crisp fuzzy logic output, perhaps rescaled to 0–100, could also be used for a thermometer-type voltage security index for control center operators.

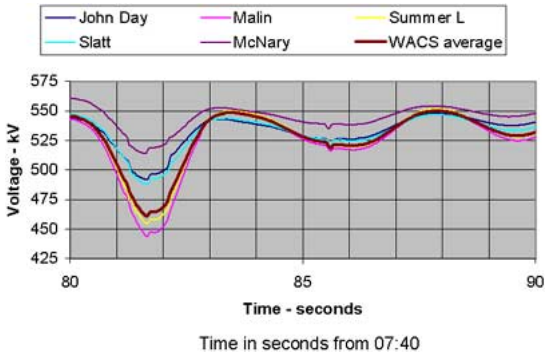

Fig. 16. Northwest voltages for first three swings.

G. Tuning, Testing, and Monitoring

Since large disturbances are rare, algorithm verification and tuning is normally via offline large-scale simulation (Appendix I). The real-time controller is tested by inputting simulation results, and also by inputting archived phasor measurements from actual events.

H. WACS Response for a Large Real Event

At 07:40:56 on Monday 14 June 2004, a short circuit occurred near the Palo Verde Nuclear Plant west of Phoenix. The fault was not completely cleared for almost 39 s! Approximately 4589 MW of generation tripped, at and near Palo Verde in the southern part of the western North American interconnection. All three Palo Verde units tripped.

Pacific intertie stability was threatened, but maintained. With one line between Oregon and California out of service, the intertie limit prior to the event was 3200 MW. North to south intertie flow swung from the initial 2750 MW to 5500 MW and settled at 4500 MW several minutes later. Malin and Captain Jack voltages near the Oregon–California border swung from the initial 548 kV to 443 kV at 07:41:21.6. Operators and an existing "response-based" scheme switched BPA series capacitors and shunt capacitor/reactor banks during the swings and the subsequent intertie power increase. The power increase is from governor action at PNW hydro plants, which carry large amounts of spinning reserve.

On 14 June, WACS was in a monitor mode at a laboratory installation 5 km from the control center and PDC. Adjusting for communications and PDC features that were not yet in service, WACS operated correctly on the forward angle swing, before voltage swing minimum, as recorded by a sequence of events recorder [25].

To further validate the WACS algorithms, we played archived data from the 14 June event into the WACS code on an offline personal computer. One parameter was retuned to increase operating speed.

Fig. 16 shows voltages that are WACS inputs and includes the weighted average voltage computed by WACS (same weights used for both algorithms). For the Vmag algorithm, the accumulator thresholds for capacitor/reactor bank switching are 525 kV and the thresholds for generator tripping are 520 kV. Accumulator setting for capacitor/reactor bank switching is 2 kV-s and accumulator setting for

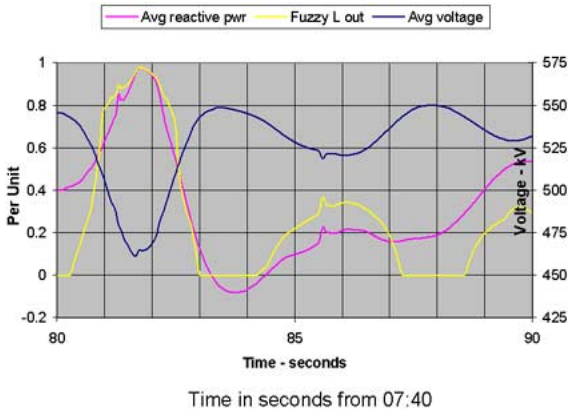

Fig. 17. $V\text{mag}Q$ fuzzy logic inputs and outputs.

generator tripping is 4 kV-s. For generator tripping, the weighted average voltage must also be below 490 kV.

For first swing stabilization, discontinuous control action should occur before the voltage minimum at around 81.6 s after 07:40. This time is estimated for the real signal without measurement delay (PMU timetags are at the last sample of the phasor computation window; the PMU uses a four-cycle moving average filter with phasors calculated over one cycle).

Using the archived data as input to the real-time code, the WACS $V\text{mag}$ algorithm output for capacitor/reactor bank switching occurs at 81.033 s after 07:40. Adding 170 ms for communications, PDC, and circuit breaker delay, switching would be at 81.203 s, or around 0.4 s before the real signal voltage minimum.

WACS $V\text{mag}$ algorithm output for generator tripping occurs at 81.233 s after 07:40. Adding 170 ms the delays, tripping would be at 81.403 s, or around 0.2 s before the real signal voltage minimum.

For the $V\text{mag}Q$ algorithm, Fig. 17 shows the weighted average voltage and weighted average reactive power that are combined using fuzzy logic. The crisp (center of gravity) fuzzy logic output is also shown. High fuzzy logic output correctly occurs for the combination of low voltage and high reactive power output. Fuzzy logic output above a threshold is accumulated. For capacitor/reactor bank switching the thresholds are 0.40 per unit (p.u.). For generator tripping, the thresholds are 0.45 p.u. Accumulator settings are 0.05 p.u.-s for capacitor/reactor bank switching and 0.2 p.u.-s for generator tripping.

The $V\text{mag}Q$ algorithm WACS output for capacitor/reactor bank switching occurs 81.033 s after 07:40 (same time as the voltage magnitude based algorithm). Adding 170 ms for communications, PDC, and circuit breaker delay, switching would be at 81.203 s, or around 0.4 s before the real signal voltage minimum.

WACS $V\text{mag}Q$ algorithm output for generator tripping occurs at 81.533 s after 07:40 (300 ms later than the voltage magnitude based algorithm). Adding 170 ms for the delays, tripping would be at 81.703 s, or around 0.1 s after the real signal voltage minimum. While this will cause a larger backswing, the generator tripping reduces intertie loading and system stress.

The 14 June massive lost of generation was well beyond planning and operating reliability criteria. While unusual, power systems *are* continuously exposed to unusual events.

If stress (Pacific intertie loading) was somewhat higher on 14 June, instability would have occurred and caused controlled islanding with massive generation/load imbalance in the importing southern island that suffered the initial 4600-MW loss. Either massive underfrequency load shedding or a widespread blackout in California, Nevada, Arizona, and New Mexico would have resulted. Stress would have been higher later in the day as temperatures and load increased.

Events like the 14 June event are exactly what WACS can protect against. Reference [25] provides more details on this event.

VII. WACS Status

Since March 2003, WACS has been installed in a laboratory with real-time phasor measurement inputs from a PDC and recording of contact outputs. Based on the following, we have demonstrated "proof of concept," and tuned and validated the real-time controller hardware and software:

- large-scale simulations including playback of simulation results into real-time code;
- monitoring of real system performance over a two-year period;
- playback of archived data into real-time code, particularly for the 14 June 2003 massive generation outage event.

With successful R&D, BPA is considering a capital budget installation for commercial use as described below.

VIII. Further Development of WACS

In parallel with the demonstration project, design requirements for permanent commercial implementation are being developed. Similar to SPS, very high reliability is required if WACS is used to increase power transfer limits. Dedicated, latest generation phasor measurement sensors likely will be required. A 60 packets per second data rate and a 60 times per second control execution rate will probably be used. Control computers will likely be at both BPA control centers, and all communications will be self-healing (geographically separated fiber-optic or digital microwave rings). The PDC function may be incorporated in the WACS computers.

After experience with single discontinuous control actions, bang–bang switching of capacitor banks can be considered for oscillation damping enhancement. Other control actions may be added, such as raising transmission voltage schedules at power plants during emergency situations; see Fig. 3. Nonlinear modulation of a static var compensator near Seattle, WA, using a voltage magnitude signal from Malin has been found effective [29] and could be implemented using WACS technology.

Many voltage and current phasor measurements plus system frequency measurements are available. Available measurements increase year by year. Binary signals from substations can be added to the phasor measurement packets.

From this data, WACS can provide monitoring and alarms for control center operators. Possibilities include event detection and monitoring of oscillation activity [30], [31, Ch. 6]. The software platform has extensive signal processing tools, and poor damping following severe disturbances is relatively easy to detect. A challenge is to minimize false alarms—logic or artificial intelligence (AI) methods applied to the large measurement base might be developed for this purpose.

Integration with other control center networks and application may offer synergies. For example, online security assessment simulations perhaps could be used for automatic tuning/learning/adaptation of WACS.

WACS is currently oriented toward improving stability of a specific interarea power transfer path. Application in other networks may be straightforward. For example, in a load area, either wide-area voltage measurements or combined voltage measurements and generator reactive power measurements could be used for reactive power compensation switching or load tripping. Such control in northern Ohio could have prevented the 14 August 2003 blackout.

Research is ongoing at WSU on further generalizing of wide-area controls to meshed networks where control strategy (measurements, disturbance classification, and generator or load tripping actions) is more difficult. WSU is also researching theoretical aspects, and use of voltage phase angles as control input. Appendices II and III describe this research.

IX. Conclusion

Automatic control experts state: "A modern view of control sees feedback as a tool for uncertainty management" [32, p. 1].

Given the many changes in the electric power industry with increasing complexity and reduced investment in transmission lines, the possibility and actual occurrences of large-scale blackouts are a worldwide concern. Clearly, new means to improve power system reliability and robustness are desirable. The addition of wide-area feedback control to frequently used wide-area feedforward control is an effective additional layer of defense against blackouts [33], as well as facilitator of electrical commerce.

WACS exploits advances in digital/optical communications and computation. Specific advantages include the following.

- Control for outages and conditions not covered by feedforward controls (SPS).
- Potentially simplifies operations for changing system conditions—currently, operators are required to reduce power transfers when unstudied conditions are encountered.
- Improved observability and controllability compared to local control. Discontinuous control reduces exposure to adverse interactions.
- Flexible, high reliability "open system" platform for rapid, low-cost control and monitoring additions, including wide-area continuous control.
- Provides a combination of reliability increase and power transfer capability increase.
- Caters to uncertainty in simulation results used to determine operating rules and limits.
- Future potential with cost reductions and further IT advances. Potential for application in meshed grid as well as intertie corridors. Control inputs and outputs may be extended over a larger geographical area such as the entire western North American power system.

Moving from WAMS to WACS (wide-area measurements to wide-area stability control) is a challenge in the new century.

Appendix I
Dynamic Simulation Methodology

Our large-scale simulations approximate the dynamic interactions between the measurement devices, communications systems, WACS actions, and power circuit breaker operations. The simulation program with WACS models changes the topology of the modeled interconnection when set conditions are met during the simulation process. For example, reactive power equipment is changed from energized to deenergized. After any change to network topology, the simulation process continues, with the effects of WACS actions fed back to the overall simulation.

The simulations start from standard data sets (base cases) compiled by the WECC. We use the General Electric PSLF/PSDS power system simulation software to solve the differential–algebraic–difference equations. WACS and other user-defined models are written in a language similar to Basic or C. A numerical integration time step of 1/4 cycle of the 60 Hz frequency (4.17 ms) is used. This is a compromise between accuracy and computing time.

Power system state variables and derived variables are calculated at every time step. Examples are substation bus voltages, transmission line currents, and frequency. Balanced conditions are assumed so calculated qualities are positive sequence values. Most controls are modeled within the main numerical integration process (digital controls other than WACS are approximated as analog controls).

We model the phasor measurements and substation to control center communications as a combination of low pass filter and pure time delay. The WACS algorithms of Section VI are modeled as described, with computations every two cycles or eight steps of the main program numerical integration. If a setpoint for either algorithm is reached for two consecutive controller cycles, a global programming variable is asserted. This represents WACS broadcasting permission for generator tripping or capacitor/reactor bank switching.

We also model actions taken at the substations and generating plants. One model deenergizes generation at selected generating plants. Propagation delays from the central site and for circuit breaker operating times are modeled.

Capacitor/reactor bank switching is locally "supervised." The signal from the central site is one input to an AND gate. The local substation bus voltage has to be below a setpoint

for a set time to satisfy the second AND gate input. We model the supervision, and also the breaker operating times.

We compare and reconcile the programming used for simulations with the real-time code. Simulation data of WACS inputs are formatted for playback into the real-time code.

APPENDIX II
THEORETICAL JUSTIFICATION FOR THE Vmag ALGORITHM

Section VI provides an overview of the WACS algorithms. The objectives are: 1) the detection and 2) the mitigation of severe disturbances in the western power system. Two algorithms, namely, Vmag and Vmag$Q$, are currently used for the real-time detection of critical large disturbances. Here we discuss a theoretical justification for the Vmag algorithm.

The Vmag algorithm relates the size of the voltage dips around the Pacific intertie lines during an event to the severity of the disturbance. Specifically, when the voltages stay below certain thresholds and when the voltage errors accumulate above the prespecified values, different control actions are initiated to mitigate the disturbance while it is still evolving. We show that the voltage dips indicate the proximity of the trajectory to the boundary of the region of attraction of the current operating point. When the trajectory stays inside the region of attraction, the system remains transient stable, which is a primary objective of the WACS control. On the other hand, if a trajectory is pushed outside the region of attraction, the system becomes transient instability and the system separates into islands.

Previous theoretical studies have shown that the region of attraction is normally bounded by: 1) the stable manifolds[1] of unstable equilibrium points (UEPs) or saddle points; 2) stable manifolds of unstable limit cycles (ULCs); and 3) segments connected with singularities of the network equations [34]. Normally, the stable manifolds of UEPs are the only ones studied in power system transient stability analysis such as in the controlling UEP algorithm in the direct stability literature [35]. Recent studies at WSU have shown that ULCs play crucial roles in anchoring the transient stability boundary in the WECC models [36], [37].

In a recent paper [37], we proposed a novel algorithm for computing the ULCs on the transient stability boundary in large-scale power system models. The algorithm was used for tracking the evolution of the unstable limit cycle on the boundary of the region of attraction for a validated model of the 10 August 1996 western blackout. A summary of the results is presented in the bifurcation diagram below. Fig. 18 shows the loci of the amplitudes of the stable and unstable limit cycles for the WECC model when the active power transfer across the intertie lines is slowly increased. The size of the limit cycles in Fig. 18 is illustrated by the high and low fluctuation values for the Malin bus voltage (California–Oregon border) for the limit cycles.

In Fig. 18, the equilibrium point becomes small-signal unstable by undergoing a subcritical Hopf bifurcation for a power transfer of 4570 MW. Specifically, ULCs anchor the

[1]Stable manifold of a UEP or a ULC denotes the set of all trajectories that converge to that UEP or ULC respectively.

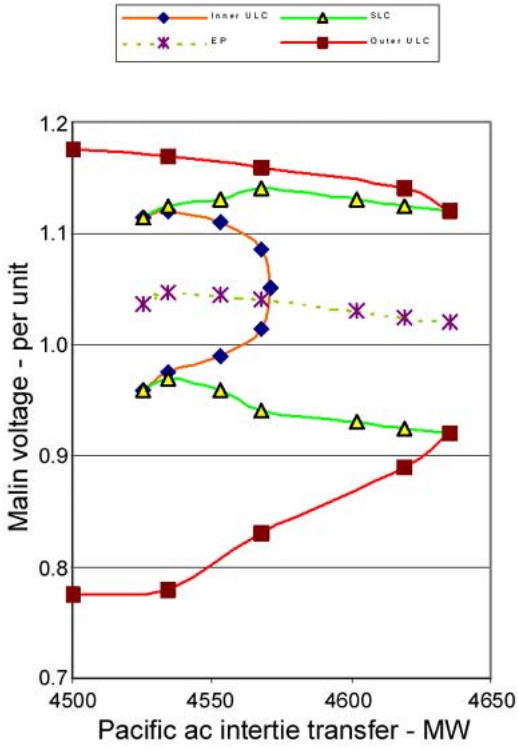

Fig. 18. Bifurcation diagram for the 10 August 1996 validated model [37].

boundary of the region of attraction for MW transfer values less than 4570 MW. For transfers below 4540 MW in Fig. 18, the ULC denoted "Outer ULC" anchors the transient stability boundary. At this ULC, the Malin bus voltage fluctuates from a low value around 0.78 p.u. (390 kV) to a high value around 1.18 p.u. (590 kV). And, interestingly, in our simulations, the size of the outer ULC does not change appreciably when the transfer decreases below 4500 MW. That is, the low voltage excursion at the Malin bus along the ULC is usually just below 400 kV for a wide range of transfer values. The same result was also observed in other WECC models in [36] and was reported in the doctoral dissertation of J. Li at WSU in 2001.

Based on these ULC computations, we conjecture that whenever the Malin bus voltage drops below 0.8 p.u. (400 kV) during a contingency, the trajectory approaches the transient stability boundary anchored by the ULC. Moreover, we can use the severity of the voltage dip at the Malin bus (or along the intertie corridor) during a disturbance to assess how close the trajectory is from the ULC on the boundary of the region of attraction. That is, the smaller the voltage swings along the corridor and the more the Malin voltage dips along the trajectory stay above 0.8 p.u., the stronger the western system is with regard to transient stability.

We employed this heuristic for assessing the dynamic security of the system by computing the severity of the intertie corridor bus voltage dips in a dynamic security optimization algorithm proposed in [38]. We showed the heuristic to be effective for improving dynamic security. The Vmag algorithm discussed in Section VI uses the same heuristic rule. We assume that the lower the voltages near the COI lines dip

during a disturbance, the closer the trajectory is to the transient stability boundary, and hence the more severe the disturbance is. Therefore, the measure of how much the intertie voltages dip toward 0.8 p.u. could be used as the heuristic for triggering the WACS control actions in the Vmag algorithm.

APPENDIX III
EXTENDING THE WACS ALGORITHMS USING PHASE ANGLES

The current algorithms used in the WACS control are based on measurements of bus voltages and generator reactive power within the BPA network. At WSU, we are developing new algorithms that detect and mitigate transient instability by utilizing the phase angle measurements of critical generator bus voltages from across the entire western system. Fast exchange of PMU measurements among WECC utilities is being pursued, and it is reasonable to assume the availability of system wide phase angle information (from specific PMU locations) in the near future.

The proposed algorithm extends the concept of the voltage-based algorithm Vmag into consideration of the phase angle measurements. At present, the algorithm analyzes the phase angles in two stages: 1) the angle stability within each control area and 2) the angle stability of the entire WECC system. The principle in each step is similar. Let us assume the availability of the phase angle measurements, say, δ_j^i, from a few key generating plants, say for $j = 1, \ldots, N^i$ in Area i. Then, we introduce the notion of the center of inertia angle reference for the area, say δ_c^i, by the rule

$$\delta_c^i = \frac{\sum_{j=1}^{N^i} \delta_j^i P_j^i}{\sum_{j=1}^{N^i} P_j^i}$$

where P_j^i denotes the current MW generation schedule at the plant j in Area i. By increasing the number of angle measurements within each area, we can improve the accuracy of the computation of the angle reference δ_c^i and we can also improve the redundancy. Similarly, the center of inertia angle reference for the entire system, denoted δ_c, can be computed with the rule

$$\delta_c = \frac{\sum_{i=1}^{N} \delta_c^i P^i}{\sum_{i=1}^{N} P^i}$$

where N is the total number of areas that are available in the control formulation, and P^i denotes the current total generation in Area i. When the representative angle δ_c^i of an area continuously increases away from the center of inertia δ_c beyond a prespecified metric, we would heuristically interpret that Area i is moving toward separation from the rest of the system. In this case, a suitable remedial action could be the tripping of generation in that area. Similarly, when the angle δ_c^i continues to decrease beyond a threshold, we would interpret that as a likely separation of Area i that could be countered by load shedding in Area i.

In our studies, we set the control trigger heuristics to be similar to the voltage error algorithm Vmag in Section VI. In the case of phase angles, we subtract the moving average value (say, $\underline{\delta_c^i} - \underline{\delta_c}$ of the relative angle $\delta_c^i - \delta_c$ from the current value by defining $\Delta\delta_c^i = (\delta_c^i - \delta_c) - (\underline{\delta_c^i} - \underline{\delta_c})$. We then accumulate two integral error terms, denoted Ω_a^i and Ω_d^i, respectively, to denote the speeding up or slowing down of Area i with respect to the center of inertia reference frame. First, the term Ω_a^i is the integral error for $\Delta\delta_c^i - \Delta\delta_a^{i*}$ whenever $\Delta\delta_c^i$ continuously stays above a threshold, say $\Delta\delta_a^{i*}$. As in Section VI, the accumulated error Ω_a^i is reset to zero whenever the angle $\Delta\delta_c^i$ drifts below $\Delta\delta_a^{i*}$. When the error Ω_a^i grows above a prespecified value, say, Ω_a^{i*}, the Area i is interpreted to be speeding away from the rest of the system and a suitable generation tripping may be initiated in that area. The value of Ω_a^{i*} will be tuned in real-time based on the current total generation and the current spinning reserve in Area i. That is, the smaller the current spinning reserve (relative to the total generation) in Area i, then the lower the threshold value for Ω_a^{i*}. The computation of the error Ω_d^i is then similar to accumulating the integral error of $\Delta\delta_c^i$ below a threshold, denoted $\Delta\delta_d^{i*}$. When the error Ω_d^i grows above the threshold Ω_d^{i*}, load tripping in Area i may be initiated to mitigate the disturbance event. The details of the algorithm will be presented elsewhere together with simulation results.

ACKNOWLEDGMENT

Many BPA engineers have assisted in the development of WACS. Dr. Y. Chen contributed to the algorithms as a Ph.D. candidate at Washington State University, Pullman.

REFERENCES

[1] P. Kundur, *Power System Stability and Control*. New York: McGraw-Hill, 1994.

[2] C. W. Taylor, *Power System Voltage Stability*. New York: McGraw-Hill, 1994.

[3] T. Van Cutsem and C. Vournas, *Voltage Stability of Electric Power Systems*. Norwell, MA: Kluwer, 1998.

[4] "Advanced angle stability controls," CIGRE, Task Force 17, Advisory Group 02, Study Committee 38, Paris, France, Brochure 155, Apr. 2000.

[5] L. L. Grigsby, Ed., *The Electric Power Engineering Handbook*: CRC Press/IEEE Press, 2001, ch. 11, Power System Dynamics and Stability.

[6] IEEE Committee Report, "A description of discrete supplementary controls for stability," *IEEE Trans. Power App. Syst.*, vol. PAS-97, no. 1, pp. 149–165, Jan./Feb. 1978.

[7] IEEE/CIGRE Joint Task Force on Stability Terms and Definitions, "Definition and classification of power system stability," *IEEE Trans. Power Syst.*, vol. 19, no. 3, pp. 1387–1401, Aug. 2004.

[8] P. M. Anderson and B. K. LeReverend, "Industry experience with special protection schemes," *IEEE Trans. Power Syst.*, vol. 11, no. 3, pp. 1166–1179, Aug. 1996.

[9] C. W. Taylor and D. C. Erickson, "Recording and analyzing the July 2 cascading outage," *IEEE Comput. Appl. Power*, vol. 10, no. 1, pp. 26–30, Jan. 1997.

[10] D. M. Kosterev, C. W. Taylor, and W. A. Mittelstadt, "Model validation for the August 10, 1996 WSCC system outage," *IEEE Trans. Power Syst.*, vol. 14, no. 3, pp. 967–979, Aug. 1999.

[11] R. L. Cresap, D. N. Scott, W. A. Mittelstadt, and C. W. Taylor, "Operating experience with modulation of the Pacific HVDC intertie," *IEEE Trans. Power App. Syst.*, vol. PAS-98, pp. 1053–1059, Jul./Aug. 1978.
[12] CIGRE, Paris, France, CIGRE 14-05, 1978.
[13] A. G. Phadke, J. S. Thorp, and M. G. Adamiak, "New measurement technique for tracking voltage phasors, local system frequency, and rate of change of frequency," *IEEE Trans. Power App. Syst.*, vol. PAS-102, no. 5, pp. 1025–1038, May 1982.
[14] R. E. Wilson, "Uses of precise time and frequency in power systems," *Proc. IEEE (Special Issue on Time and Frequency)*, vol. 79, no. 7, pp. 1009–1018, Jul. 1991.
[15] IEEE Power Syst. Relaying Comm. (WG H-7, A. G. Phadke, Chairman), "Synchronized sampling and phasor measurements for relaying and control," *IEEE Trans. Power Del.*, vol. 9, no. 1, pp. 442–452, Jan. 1994.
[16] IEEE Power Syst. Relaying Comm. (WG H-8, K. E. Martin, Chairman), "IEEE standard for synchrophasors for power systems," *IEEE Trans. Power Del.*, vol. 13, no. 1, pp. 73–77, Jan. 1998.
[17] G. Benmouyal, E. E. Schweitzer, and A. Guzman, "Synchronized phasor measurement in protective relays for protection, control, and analysis of electric power systems," presented at the 29th Annu. Western Protective Relay Conf., Spokane, WA, 2002.
[18] J. Hauer, D. Trudnowski, G. Rogers, B. Mittelstadt, W. Litzenberger, and J. Johnson, "Keeping an eye on power system dynamics," *IEEE Comput. Appl. Power*, vol. 10, no. 4, pp. 50–54, Oct. 1997.
[19] I. Kamwa, R. Grondin, and Y. Hebert, "Wide-area measurement based stabilizing control of large power systems—a decentralized/hierarchical approach," *IEEE Trans. Power Syst.*, vol. 16, no. 1, pp. 136–153, Feb. 2001.
[20] J. F. Hauer and C. W. Taylor, "Information, reliability, and control in the new power system," in *Proc. 1998 American Control Conf.*, vol. 5, pp. 2986–2991.
[21] J. Lambert, A. G. Phadke, and D. McNabb, "Accurate voltage phasor measurement in a series-compensated network," *IEEE Trans. Power Del.*, vol. 9, no. 1, pp. 501–509, Jan. 1994.
[22] C. W. Taylor, V. Venkatasubramanian, and Y. Chen, "Wide-area stability and voltage control," presented at the Seventh Symp. Specialists in Electric Operational and Expansion Planning (VII SEPOPE), Curitiba, Brazil, 2000.
[23] C. W. Taylor and R. E. Wilson, "BPA's Wide-Area stability and voltage Control System (WACS): overview and large-scale simulations," presented at the Sixth Symp. Specialists in Electric Operational and Expansion Planning (IX SEPOPE), Rio de Janeiro, Brazil, 2004.
[24] R. E. Wilson and C. W. Taylor, "Using dynamic simulations to design the wide-area stability and voltage control system (WACS)," presented at the IEEE Power Engineering Soc. Power System Conf. Exposition, New York, 2004.
[25] C. W. Taylor, D. C. Erickson, and R. E. Wilson, "Reducing blackout risk by a wide-area control system (WACS): Adding a new layer of defense," in *Proc. 2005 Power System Computation Conf.*, submitted for publication.
[26] U.S.-Canada Power System Outage Task Force, *Final Report on the August 14, 2003 Blackout in the United States and Canada: Causes and Recommendations*, Apr. 2004.
[27] National Instruments [Online]. Available: http://www.ni.com
[28] D. Kosterev, "Design, installation, and initial operating experience with line drop compensation at John Day powerhouse," *IEEE Trans. Power Syst.*, vol. 16, no. 2, pp. 261–265, May 2001.
[29] V. Venkatasubramanian, K. W. Schneider, and C. W. Taylor, "Improving Pacific inter-tie stability using existing static VAR compensators and thyristor controlled series compensation," in *Proc. Bulk Power System Dynamics and Control IV—Restructuring*, 1998, pp. 647–650.
[30] J. F. Hauer and F. Vakili, "An oscillation trigger for power system monitoring," *IEEE Trans. Power Syst.*, vol. 5, no. 1, pp. 74–79, Feb. 1990.
[31] J. F. Hauer *et al.*, "A Dynamic Information Manager for Networked Monitoring of Large Power Systems," EPRI, Palo Alto, CA, Final Rep. TR-112 031, 1999.
[32] R. M. Murray. (2002, Jun.) Control in an information rich world. [Online]. Available: http://www.cds.caltech.edu/~murray/cdspanel/report/cdspanel-15aug02.pdf
[33] C. W. Taylor, "Improving grid behavior," *IEEE Spectrum*, vol. 36, no. 6, pp. 40–45, Jun. 1999.
[34] V. Venkatasubramanian, H. Schattler, and J. Zaborszky, "A taxonomy of the dynamics of large differential-algebraic systems," *Proc. IEEE*, vol. 83, no. 11, pp. 1530–1561, Nov. 1995.
[35] V. Vittal and A. A. Fouad, *Power System Transient Stability Analysis Using the Transient Energy Function Method*. Englewood Cliffs, NJ: Prentice-Hall, 1991.
[36] J. Li and V. Venkatasubramanian, "Study of unstable limit cycles in power system models," *IEEE Trans. Power Syst.*, submitted for publication.
[37] V. Venkatasubramanian and Y. Li, "Analysis of 1996 western American electric black-outs," presented at the Bulk Power System Dynamics and Control VI Conf., Cortina, Italy, 2004.
[38] Y. Li and V. Venkatasubramanian, "Coordination of transmission path transfers," *IEEE Trans. Power Syst.*, vol. 19, no. 3, pp. 1607–1615, Aug. 2004.

Carson W. Taylor (Fellow, IEEE) received the B.S.E.E. degree from the University of Wisconsin, Madison, in 1965 and the M.S. degree in electric power engineering from Rensselaer Polytechnic Institute, Troy, NY, in 1969.

He joined the Bonneville Power Administration (BPA), Portland, OR, in 1969. He is now Principal Engineer in Transmission Operations and Planning, where he is developing wide-area voltage and stability controls. Besides his BPA work, he consults and teaches power system engineering. In 1986, he established *Carson Taylor Seminars*. He has presented 72 seminars in 17 countries. He is the author of the book *Power System Voltage Stability* (New York: McGraw-Hill, 1994). The book is translated into Chinese. Mr. Taylor has authored or coauthored many IEEE and CIGRE papers. His interests include power system control and protection, system dynamic performance, ac/dc interactions, and power system operations and planning.

Mr. Taylor is a Member of the U.S. National Academy of Engineering and a Distinguished Member of CIGRE. He is Past Chairman of the IEEE Power Engineering Society (PES) Power System Stability Controls Subcommittee. He is Convenor of three CIGRE task forces on power system voltage and angle stability.

Dennis C. Erickson (Fellow, IEEE) received the B.S. degree in general engineering at the University of Portland, Portland, OR, in 1968 and has continued his education through postgraduate programs and specialized courses.

During his tenure at the Bonneville Power Administration, Portland, (1965–2000), he designed precision time dissemination and frequency measurement systems for real-time power system control applications, and evaluated research on free space optical and millimetric communications systems. He was the Principal Engineer on BPA's automatic overhead transmission line fault locator network and developed several major innovations in that field. He developed novel high voltage measurement systems employing electrooptic and magnetooptic dielectric sensors, and high precision wide bandwidth analog and digital fiber-optic instrumentation links. From 2000 to 2002, he was with Quantum Controls Inc. as a Senior Technical Consultant. At present, he is with Ciber Inc., Beaverton, OR, as a Chief Systems Engineer designing advanced power system control systems and data acquisition, dissemination, and analysis systems. He holds one patent in the field. He is the author of over 20 technical papers, including papers on optical sensors and multifunctional data acquisition techniques.

Mr. Erickson is the Founding Chairman of the Fiber Optics Subcommittee of the IEEE Power Engineering Society (PES) Power System Communications Committee.

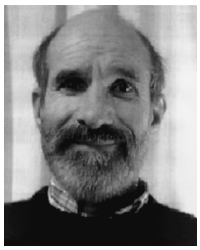

Kenneth E. Martin (Senior Member, IEEE) received the B.S.E.E. degree from Colorado State University, Fort Collins, in 1970 and the M.A. degree in mathematics from the University of Washington, Seattle, in 1974.

He served in the U.S. Army from 1970 to 1972, primarily designing instrumentation at the Yuma Proving Ground. He joined the Bonneville Power Administration, Portland, OR, in 1975 where he has worked with system protection, control systems, telecommunications, and instrumentation. He is currently Principal Engineer in the Measurement Systems group. He has authored or coauthored numerous technical papers and made technical presentations in several countries. His main interests are global positioning system-based timing systems and wide area, real-time power system measurements, particular phasor measurements.

Mr. Martin is a Registered Professional Engineer in Washington State. In 2003 he received the BPA Eugene C. Starr award for Technical Achievement. He is a Member of the IEEE Power Engineering Society (PES) Power System Relay Committee and the Relay Communications Subcommittee. He chairs the Synchrophasor Standard working group.

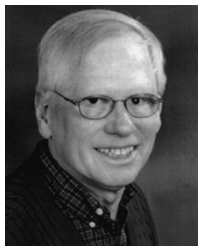

Robert E. Wilson (Senior Member, IEEE) received the B.S.E.E. degree from the University of Nebraska, Lincoln, in 1969, the M.S. degree in electrical engineering and the M.A. degree in mathematics from the University of Arizona, Tucson, in 1973 and 1980, respectively, and the M.E. and Ph.D. degrees in electrical engineering from the University of Idaho, Moscow, in 1989 and 1992, respectively.

From 1980 to 1990, and again from 1994 to the present, he worked for the Western Area Power Administration, U.S. Department of Energy, Lakewood, CO. From 1990 to 1992 he was the Washington Water Power Fellow at the University of Idaho. From 1992 to 1994, he was the first Nicholson Visiting Assistant Professor of Electrical Engineering, University of Wyoming, Laramie. From 2002 to 2003, he worked for the Bonneville Power Administration, Portland, OR, via an interagency agreement. He has authored or coauthored many technical papers. He has studied the applications of precise time and frequency in power systems since 1985. He is currently studying advanced control systems for the western North American power grid and advanced methods of data display and methods to transport renewable energy into California.

Dr. Wilson is a Registered Professional Engineer in the state of Colorado. He was a Member of the IEEE Power Engineering Society (PES) Power System Relay Committee and the IEEE Working Group on Phasor Measurements, and was Cochair of a task force that wrote one chapter in the IEEE Special Publication *Modeling and Analysis of System Transients Using Digital Programs* (Pub. No. 99-TP-133-0, 1999).

Vaithianathan Venkatasubramanian received the B.E. (honors) degree in electrical and electronics engineering from the Birla Institute of Technology and Science, Pilani, India in 1986 and the M.S. and D.Sc. degrees in systems science and mathematics from Washington University, St. Louis, MO, in 1989 and 1992, respectively.

He is a Professor of Electrical Engineering and Computer Science at Washington State University, Pullman, WA. His research interests are power system stability and control, and nonlinear system theory.